Evaluation of Physical Capture Efficiency and Disinfection Capability of an Iodinated Biocidal Filter Medium

Shanna Ratnesar-Shumate[1], Chang-Yu Wu[2*], Joe Wander[3], Dale Lundgren[2], Sam Farrah[4], Jin-Hwa Lee[2], Prinda Wanakule[5], Matthew Blackburn[6], Mei-Fang Lan[7]

[1] The Johns Hopkins University Applied Physics Laboratory

[2] University of Florida, Department of Environmental Engineering Sciences

[3] Air Force Research Laboratory, Tyndall Air Force Base

[4] University of Florida, Department of Microbiology and Cell Sciences

[5] University of Florida, Department of Agricultural and Biological Engineering

[6] University of Florida, Department of Chemical Engineering

[7] University of California – Davis, Department of Psychiatry and Behavioral Sciences

Abstract

Poly(styrene–divinylbenzene)-4-(methyltrimethylammonium) triiodide (PMT) has recently been applied onto nonwoven air filter media to purportedly combine filtration and iodine disinfection to achieve enhanced attenuation of viable airborne pathogens without aggravating the pressure drop of the medium. This paper reports and compares the physical capture efficiency and biological removal efficiency of the novel biocidal filter medium. During challenges with inert fluorescent particles, both iodine-treated and untreated media displayed statistically equivalent physical capture efficiencies > 97%, and typically > 99%. The pressure drag (3.2 kPa·s/m) was less than 10% that of a glass fiber HEPA (38 kPa·s/m) medium. Biological disinfection by the media was evaluated using aerosols containing *M. luteus* and *E. coli* vegetative bacterial cells. Biological removal efficiency (99.997%) was observed to be two logs greater than inert particle capture. Viable penetration through the biocidal filters was observed in only two of 10 experiments. The results suggest that an antimicrobial-coated filter medium can provide effective protection against airborne pathogens with a significantly lower pressure drop than that imposed by conventional high-efficiency filtration systems. A near-contact mechanism is proposed in which the distances of nearest approach to treated fiber surfaces as a microbe penetrates through the filter define the probability that charge sites on the microbe's surface will capture enough iodine molecules from triiodide complexes at the surfaces to terminate viability.

Keywords: Bioaerosol; Disinfection; Filtration; Iodine; Pressure drag.

*Corresponding author. Tel.: 352-392-0845; Fax: 352-392-3076

E-*mail address*: cywu@ufl.edu

INTRODUCTION

Concern excited by press coverage of the

anthrax incident in 2001 escalated the emerging threat of bioterrorism into a great concern for national security. Among the various modes available for staging a biological attack, aerosolization is considered the most effective for dispersing biological agents over a wide area in a short time (Kortepeter and Parker, 1999). The pandemic Severe Acute Respiratory Syndrome (SARS) and the impending threat of avian flu are natural examples illustrating profound, everyday impacts of bioaerosols on public health.

The NIOSH-approved N95 filtering facepiece respirator is the protective device most commonly used by medical personnel and first responders to reduce the risk of inhaling particulate hazards. Since the introduction of the N95 category, reports examining efficacy of protection afforded by such devices based on 95% capture (at 300 nm) efficient media against inert particles (Qian *et al.,* 1998; Richardson *et al.,* 2006; Rengasamy *et al.,* 2007) and against aerosols containing MS2 coli phage (Brosseau *et al.,* 1997; Balazy *et al.,* 2006) showed less than 2% penetration at airflow rates near 30 L/min for the most penetrating size (~ 50 nm), but penetration increased to 5% at 85 L/min. The capture efficiency of filters is known to depend on several factors including the size of the challenging aerosols, the filter fibers, the velocity of airflow through the filter, and the presence or absence of electric charge on the fibers or particles (Hinds, 1999a).

A more efficient technology to remove bioaerosols from air is the High Efficiency Particulate Air (HEPA) filter, which is rated to remove 99.97% of 300-nm particles. According to OSHA, a NIOSH certified N, R, or P100 class respirator is equivalent to a HEPA. Brosseau *et al.* (1997) reported a steep decrease in efficiency of removal of *Mycobacterium abscessens* by HEPA filters as air flowrate increased. Another associated issue of HEPA filters is increased breathing resistance as flow rate increases, which can be detrimental to the respirator user.

Another consideration in bioaerosol protection is viability of collected microorganisms. Under favorable nutrition and moisture conditions, a significant fraction of airborne microorganisms can remain viable after collection on filtration devices as they load, and microbial growth can occur on filters. For example, molds are able to grow on fibrous media if provided with 70–80% relative humidity and atmospheric dust (Maus *et al.,* 2000). Subsequent re-entrainment from filter media is then possible, *e.g.*, the re-entrainment of MS2 virus from filter media described by Richardson *et al.* (2006). These functional limitations suggest that some augmentation of conventional filtration might lead to better technologies for respiratory protection.

The halogens iodine and chlorine are antimicrobial agents of great importance. Halogen disinfection is a method of chemical sterilization in which oxidation of cell constituents and halogenation of cell proteins occurs (Prescott *et al.,* 2002). Iodine is widely used as a disinfectant for potable and on-site water treatment, and is known for its stable chemical storage characteristics (Brion and Silverstein, 1999). Elemental iodine (I_2) is not

highly soluble in water but may be introduced by heat vaporization, crystal dissolution, oxidation of iodide (I^-) ion, and release from iodine-containing resins or from the direct addition of high-strength iodine/alcohol solutions or solutions of triiodide (I_3^-) ions (Black *et al.,* 1968). I_2 is more soluble in solutions of iodide ion, forming the "classical" (Cotton *et al.,* 1999) linear (Swenson and Kloo, 2002) I_3^- ion, which was reported (Carroll, 1955) to be a much less-effective antiseptic than I_2 in water. The $I^- + I_2^- \rightarrow I_3^-$ reaction is reversible (Jones, 1930). Rates of exchange reactions of I_3^- with I_2 (Katzin and Gerbert, 1955) and with I^- (Ruff *et al.,* 1972) have been measured, and higher homologues have been observed in the solid state, *e.g.*, I_5^- (Teitelbaum *et al.,* 1980) with I_3^- and higher homologues (Saenger, 1984; Yu *et al.,* 1996) in the starch–iodine complex and in charge transfer complexes of iodine with polynuclear aromatic hydrocarbons (Teitelbaum *et al.,* 1980) and with metal α-diketonates (Cowie *et al.,* 1979).

I_3^- and I_5^- ions bind to quaternary ammonium anion exchange resins and form stable complexes (Chang, 1958; Berg *et al.,* 1964; Taylor *et al.,* 1970; Brion and Silverstein, 1999). Nonspecific antimicrobial activity of these complexes has been studied extensively in water (Taylor *et al.,* 1970; Fina *et al.,* 1982), and a patent was issued (Lambert and Fina, 1975) for the preparation and use of a 4-trimethylammoniummethyl derivative (PMT, Fig. 1) of poly(styrene–divinylbenzene) as a broad-spectrum, demand-type disinfectant for bacteria in water, in which spontaneous release of iodine was shown to be very slow and deduced to be strongly enhanced when reactive species are encountered. This concept was adopted for water disinfection aboard spacecraft (Marchin *et al.,* 1997).

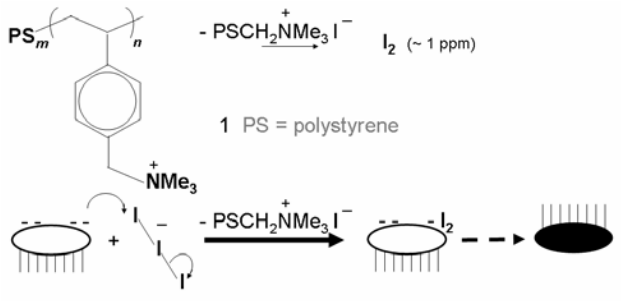

Fig. 1. Poly(styrene–divinylbenzene)-4-(trimethylammonium)methyl triodide (1) and its conceptual mechanism for disinfecting microorganisms.

A patent by Messier (2000) extended the use of PMT to air filtration and claimed that such resins can effect efficient, nonspecific attenuation of viable microorganisms in air under various conditions. Air filtration media coated with PMT have also been shown to attenuate viability of MS2 bioaerosols by a 2-log factor compared to untreated HEPA (Heimbuch *et al.,* 2004) media and to P95 (Heimbuch and Wander, 2006) media (the P95 class performs to the N95 standard and is also oil resistant); however, the aerosol challenges applied in these demonstrations were not experimentally characterized. This study was undertaken to isolate the mechanical and chemical or biological processes acting in a P95 medium by first characterizing the mechanical particle removal efficiency (PRE) of the untreated and treated media with an inert aerosol. Experiments were then

Table. 1. Experimental conditions of phase I – physical removal efficiency and phase II – biological removal efficiency.

Phase	Test Particles	Challenge Flow Rate (L/min)	Number of Replicates	Upstream Test Filter	Filter Thickness (mm)	Downstream Filter
I	Ammonium Fluorescein	13	3	Iodine-treated filter	1	Glass fiber filter
		15	3		1	
		21	3	Untreated filter	1	
		15	3	Glass fiber filter	2	
II	*M. luteus*	15	6	Iodine-treated filter	1.5	N/A
	E. coli		4			

conducted to measure the viable bacterial removal efficiency (vBRE) using two types of vegetative bacterial cells. Finally PRE and vBRE were compared to extract the attenuation of viability caused by the iodinated antimicrobial coating. To generalize the comparison, the pressure drag of an iodinated P95 medium was compared to that of a glass fiber HEPA filter, and the effects of flow rate and filter thickness were investigated.

METHODS

The experiments were carried out in two phases. In Phase I, the PRE was evaluated using fluorescent aerosols. In Phase II, two types of vegetative cells were challenged to assess the filter's vBRE. The same experimental system was used in both phases. The experimental conditions for both phases are summarized in Table 1.

Experimental set-up

Fig. 2 shows the schematic of the experimental set-up. Aerosols were generated for Phase I experiments using a Six-Jet Collison Nebulizer (Model CN25, BGI Inc.) at a flow rate of 10 L/min. Filtered compressed air was dried using a diffusion dryer and introduced into a dilution chamber at twice the flow rate of the aerosol generation to evaporate the water content of the aerosol droplets (May, 1972). Filters for Phase I experiments were tested in series. In order to achieve the desired challenge flow rates of 13, 15, and 21 L/min through the test filters, excess air was diverted from the main air stream by vacuum. Additional particle-free dry air was added to the air stream after the test filters to maintain the required flow rate of 28.3 L/min for the cascade impactor.

For Phase II, bioaerosols were generated using the nebulizer at a flow rate of 7 L/min and a dilution air flow of 13 L/min. Filters (or

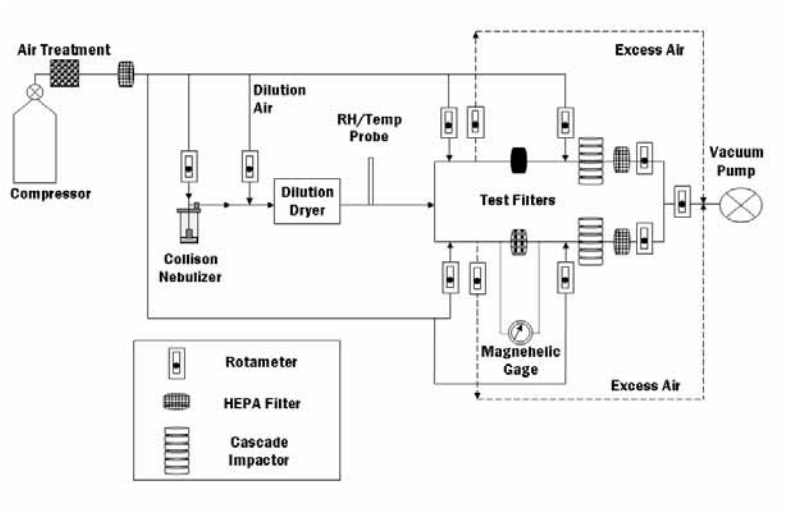

Fig. 2. A schematic diagram of the experimental set-up.

empty filter holder in the control runs) for Phase II experiments were tested in parallel. The air flow was split into two equal air streams and additional air was introduced downstream of the dilution drier to maintain 15 L/min passing through both the test filter and the control. Relative humidity and temperature of the air stream were monitored (HX 94, Relative Humidity/Temperature Transmitters, Omega Engineering) upstream of the filters. A Magnehelic gage reading 0–10 in H_2O was employed to measure the pressure drop across the resin/iodine filters. A reading was taken every minute for each run. Penetrating aerosols leaving the test filters were captured and classified by particle size on a six-stage Andersen viable impactor (Model #10-820). To maintain the impactor's required nozzle-to-surface distance, plates were mounted within Petri dishes at the design height. Flow rates through the filters and cascade impactors were measured and maintained using calibrated rotameters and a background vacuum as depicted in (Fig. 2).

Test particles

In Phase I, ammonium fluorescein particles were employed to evaluate the physical capture efficiency of the filters. Fluorescence was considered because of its lower detection limit compared to gravimetric measurements. A 6.75-g/L fluorescein solution in 0.1 *N* NH_4OH was aerosolized by the Collison nebulizer. The mass median diameter of the dry fluorescein particles was calculated to be ~ 0.27 μm, based on the following equation (Hinds, 1999b):

$$d_a = d_d \left(F_v\right)^{1/3} \tag{1}$$

where d_d is the mass median diameter of the atomized droplet (~ 3 μm; (May, 1972)) and F_v is the volume fraction of fluorescein in the solution.

In Phase II, nonpathogenic microorganisms for bioaerosol challenges were selected based on several factors. *Escherichia coli* is a Gram-negative, rod-shaped bacterium that ranges in size from 2 to 3 μm in length and 0.25 to 1 μm

in diameter. The strain used was obtained from the Water Reclamation Facility at the University of Florida. The samples obtained were inoculated and maintained on Difco tryptic soy agar and grown at 33ºC prior to sampling. *Micrococcus luteus* is another frequently used representative bioaerosol (Wake *et al.,* 1997; Li and Lin, 2001; Agranovski *et al.,* 2003). *M. luteus* cells are Gram-positive, non-motile, nonsporulating, round bacteria normally found in clusters or tetrads. The individual cells are 0.9 to 1.8 μm in diameter (Wake *et al.,* 1997). *M. luteus* samples were obtained from the University of Florida, Department of Microbiology and Cell Sciences. Cells were inoculated on standard nutrient agar (Difco 0001) and maintained at 33ºC prior to sampling. Note that the purpose of this investigation was to characterize the interaction between filtration media and generically delivered aerosols containing viable microbes. Accordingly we used a simple aqueous dispersant that creates conditions favorable for survival of the organisms in air, rather than the actual or simulated human fluids that one would employ in a study considering factors relating to contagion. Prior studies (Wake *et al.,* 1997; Crook *et al.,* 1998) have shown that Ringer's solution can maintain the viability of stressed bacteria used in aerosol studies. Hence, bioaerosol suspensions for use in the Collison nebulizer were created by washing bacterial cells off agar slants using 1 mL of 25% Ringer's solution (Fisher, S77939). The slants were agitated for 20 s using a standard vortex, and varying amounts of each sample were aseptically pipetted out of the slant test tubes and into Ringer's solution contained in the nebulizer reservoir for each experiment.

Test filter

Flat sheet P95 filter media were provided by Triosyn Corp. P95 filters are defined as those with 95% efficiency when challenged with aerosol of 185 nm count median diameter (CMD) (equivalent to 0.3 μm mass median diameter (MMD) with a geometric standard deviation of 1.5) (NIOSH, 2005). The iodinated resin is produced by thermally fusing pure iodine crystals with a quaternary anion exchange polymer under high pressure (Messier, 2000). Iodine-treated and untreated filters of 1 mm thickness were tested for physical capture efficiency. Heavier filters of 2 mm thickness were used to evaluate the effect of depth. The bioaerosol experiments were conducted using medium-depth filters with an approximate thickness of about 1.5 mm.

The filter media tested were 47 mm in diameter (area 17.35 cm^2). A common respirator cartridge has a cross-sectional area of approximately 100 cm^2 (Di Ionno and Messier, 2004), and the flow rate used in NIOSH certification testing is 85 L/min (NIOSH, 2005; Rengasamy *et al.,* 2007). Accordingly, the flow rate used for testing the 47-mm filter was scaled down to 15 L/min to produce a similar face velocity. Two other flow rates, 13 and 21 L/min, were used to evaluate the effect of flow velocity. Bioaerosol challenges were conducted only at 15 L/min air flow rate.

Experimental procedure

Phase I

Each experiment was run for 15 minutes. This amount of time was shown to be sufficient to deliver a measurable amount of fluorescent particles for evaluation, while not causing a mound effect due to accumulation of particles under each impactor jet, which might alter the collection characteristics of the impactor. After collection, the individual stages containing fluorescein particles were rehydrated in aqueous 0.1 *N* NH_4OH solution. They were then treated with 20 mL of methylene chloride to dissolve the grease coating on each plate and sonicated for 10 minutes. Twenty mL of 0.1 *N* NH_4OH was added to each sample after sonication and poured into a test tube. Due to the immiscibility of methylene chloride and aqueous ammonium hydroxide, a fluorescein–ammonium hydroxide solution separated to the top of each sample while the methylene chloride, containing the grease, sank to the bottom. The top layer of each sample was then pipetted into a quartz cuvette for analysis (Vanderpool *et al.,* 1987).

Mass concentrations of fluorescein solution from each stage were measured using a Sequoia–Turner 112 Digital Filter Fluorometer (G.K. Turner Associates). A calibration of concentration vs. fluorometer reading was performed using samples of known fluorescein concentration in 0.1 *N* NH_4OH for fluorometer range settings of 1X, 3X, 10X, and 30X. Accuracy was maintained by selecting range settings that best suited the concentration of the solution being analyzed.

Several factors may skew the results of fluorometric analysis, including fluorescence given off by reagents, filter substances reacting with chemicals, or flaws within different cuvettes used in analysis. For this reason, several background tests for the various filter media were conducted. The results indicate that there was no interference with fluorescence analysis by the glass fiber and untreated filters. Variations in the optical properties of each cuvette were also shown to have negligible effect on data reproducibility. A maximum standard deviation of only 0.8% was observed at 500 μg/L based on 36 fluorometric readings of different cuvettes oriented at different directions and at differing concentrations. However, a negative interference was observed for the iodine-treated filters. The interference was attributed to oxidation and/or iodination of fluorescein in the rehydrated filter solution, and it resulted in a lower apparent concentration (Naim *et al.,* 1986). A concentration-based interference curve was therefore established to adjust the values measured.

Phase II

To measure the inlet concentration of bioaerosols entering the test system vs. those captured by filtration, two impactors were used in parallel. One impactor contained an iodine-treated filter upstream, whilst the other contained no filter upstream as positive control. Although the impact of the variation of the microorganism's viability during nebulizer operation is a concern during bioaerosol generation, such a concern is irrelevant to our study as we were comparing two systems in parallel, *i.e.*, the changes were equal. The inlet concentrations were measured by the positive

control stream for the first and last five minutes of each experiment using Petri dishes on all six stages of the impactor.

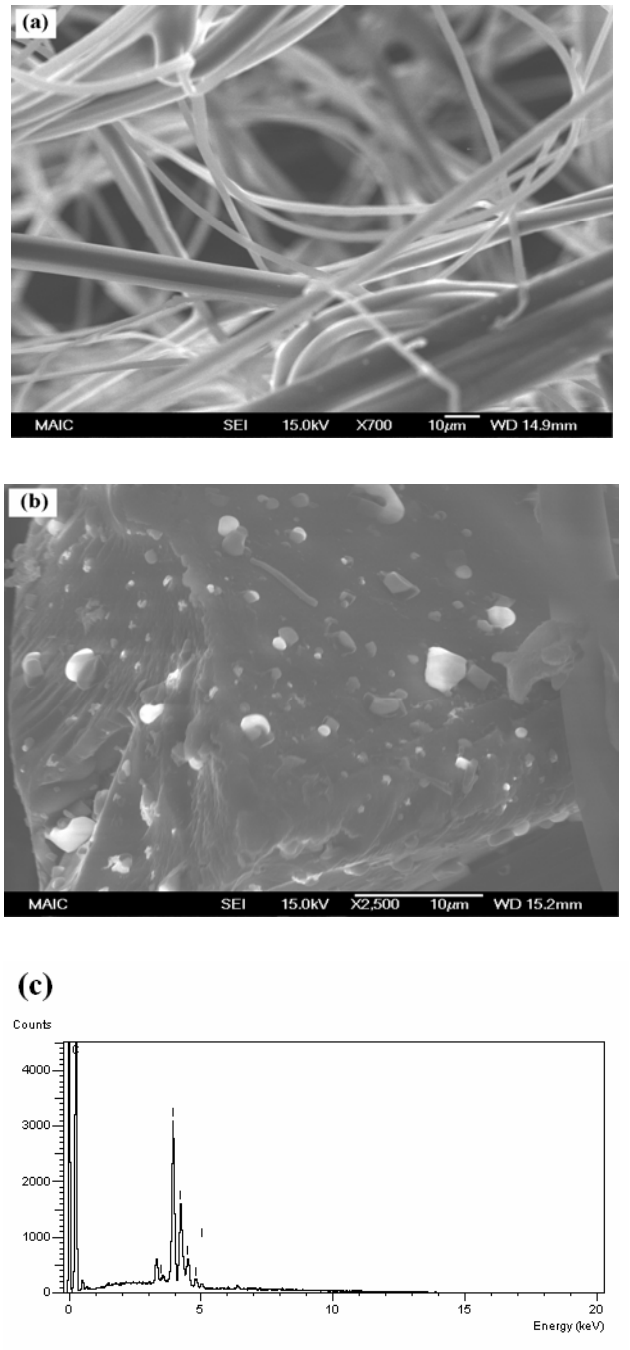

Fig. 3. (a) SEM image of untreated filter at 700X; (b) SEM image of enlarged fleck at 2500X; (c) EDX spectrum of (b).

Due to the very low penetrating concentration, the bioaerosol was collected on only one Petri dish on stage 6 (last stage) from the experimental stream. Every 20 minutes throughout the 2-h run, the outlet Petri dishes were changed out to prevent desiccation of the agar surface. After each plate was removed from the impactors, it was labeled and placed in an incubator at 33ºC for 24–36 h. The optical count of the colony-forming units (cfu) that impacted onto an agar surface was corrected following the Positive Hole Method (Thermo Electron Corp., 2003).

Immediately after the filtration experiment, the test filter was subjected to a vortexing experiment to determine the viability of the bacteria collected on the filter. The filter was immersed in 40 mL of 25% Ringer's solution and agitated with a vortex mixer (Model M16715, Barnstead). After vortexing for 1 min, 1 mL of sample was withdrawn for measuring the viability of the extracted bacteria in the original solution, and another 1 mL was withdrawn and measured after appropriate dilution. The same procedure was repeated after 2, 3, 5, and 10 mins of vortexing time, without changing the solution. The effect of vortexing on the viability of bacteria was also investigated by following the same vortexing procedure with a known concentration of bacteria sump, although vortexing alone was found to exert no effects on the cell's viability.

Statistical analysis of data

Three controls (no filter upstream) and three experimental runs were conducted separately

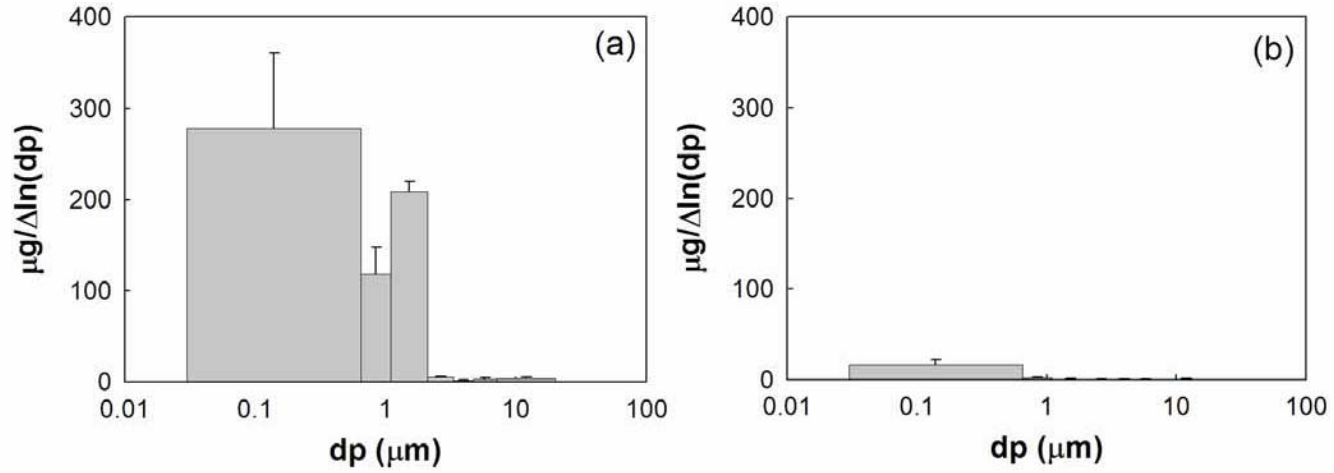

Fig. 4. Mass size distribution of ammonium fluorescein particles for Phase 1 at 15 L/min: (a) control experiments, (b) with an iodinated filter upstream.

for each flow rate tested. A linear least squares method was used to correlate the data (Vining, 1998). This method considers the data points assessed during the experiments and finds the best straight-line equation to represent all combinations of the data. The *x*-axis represents the control mass fraction measured for each stage for this analysis, and the *y*-axis represents the difference between the control mass fraction and the penetration mass fraction for each stage. The efficiencies reported were the slopes calculated based on the least squares methods, and the error ranges reported were the standard errors for the *y* estimates.

Filter morphology analysis

Microscopic images of the filters before and after sampling were taken using scanning electron microscopy (SEM) to evaluate any differences in morphology due to treatment or use of the filters. Elemental analysis of objects magnified with SEM was performed using energy dispersive X-ray spectroscopy (EDS).

RESULTS

Morphology analysis of filter media

Untreated filters were analyzed via SEM prior to experimentation (not shown). A dense woven structure of long fibers of different thickness was observed by visual analysis. Iodine-treated filters were also analyzed via SEM prior to experimentation (Fig. 3a and 3b). Small dark flecks were observed around the outer perimeter of the filter surfaces. The EDS analysis of the small flecks indicated the presence of iodine (Fig. 3c). Similar results were observed for the EDS taken of the filter fibers (not shown), demonstrating the presence of iodine on the fiber surface.

Phase I – physical capture

The mass size distribution of particles produced in the system reaching the point of filtration was determined during control runs using no filter upstream of the impactor. Fig. 4a shows the size distribution at 15 L/min as an

example. The shape of the distribution of other flow rates had a similar pattern, while the total mass increased as the flow rate increased. The majority of the fluorescent particles were collected on the downstream filter stage (< 0.65 μm) and 5th and 6th stages (2.1–1.1 and 1.1–0.65 μm, respectively) for each flow rate. The data for stages 1 to 4 were not used due to the low concentrations of detectable particles. The mean corresponding total mass concentrations were 1.33 x 10^7, 2.14 x 10^7, and 4.03 x 10^7 μg/m^3 for 13, 15, and 21 L/min, respectively.

Table 2 summarizes the PRE at each stage of the impactor for iodine-treated and untreated filters at different flow rates. Fig. 4b shows, as an example, the mass size distribution downstream from an iodinated resin filter. As shown, significant capture (greater than 97%) was observed for both the iodine-treated and untreated filters tested for stages 5 and 6 and for the downstream filter (DF). DFs were visually analyzed after sampling and rehydration. It was observed that some amount of fluorescein was not captured by the upstream iodinated resin filter. No fluorescence was observed on the downstream filters when similar experiments were performed using glass fiber filters (Millipore, Lot # H3NN53241) upstream, verifying that the glass fiber filters have a higher PRE for fluorescent particles than the iodinated resin P95 filters do. Rehydrated solutions in test tubes were also visually analyzed prior to pipetting into cuvettes. No visible fluorescence was observed when glass fiber filters were located upstream, whereas visible fluorescence could be seen from the iodinated resin samples.

Table. 2. Physical capture efficiency (mean ± σ) of iodinated resin filters per stage.

	Stage# (Size range, μm)			
Sample, Filter thickness, Flow rate	5 (2.1–1.1)	6 (1.1–0.65)	DF (0.65–0.03)	Total (2.1–0.03)
Treated, 1 mm, @ 13 L/min	99.86 ± 0.011	99.96 ± 0.029	99.22 ± 0.167	99.34 ± 0.118
Untreated, 1 mm, @ 13 L/min	99.91 ± 0.004	99.79 ± 0.026	99.12 ± 0.184	99.62 ± 0.830
Treated, 1 mm, @ 15 L/min	99.81 ± 0.005	99.21 ± 0.046	96.84 ± 0.063	97.32 ± 0.381
Untreated, 1 mm, @ 15 L/min	99.89 ± 0.033	99.87 ± 0.023	99.38 ± 0.101	99.43 ± 0.083
Treated, 1 mm, @ 21 L/min	99.99 ± 0.000	99.51 ± 0.020	98.85 ± 0.149	99.01 ± 0.088
Untreated, 1 mm, @ 21 L/min	99.93 ± 0.032	99.53 ± 0.031	98.95 ± 0.263	99.07 ± 0.191
Thick Treated, 2 mm, @ 15 L/min	99.94 ± 0.002	99.97 ± 0.002	99.50 ± 0.126	99.56 ± 0.090

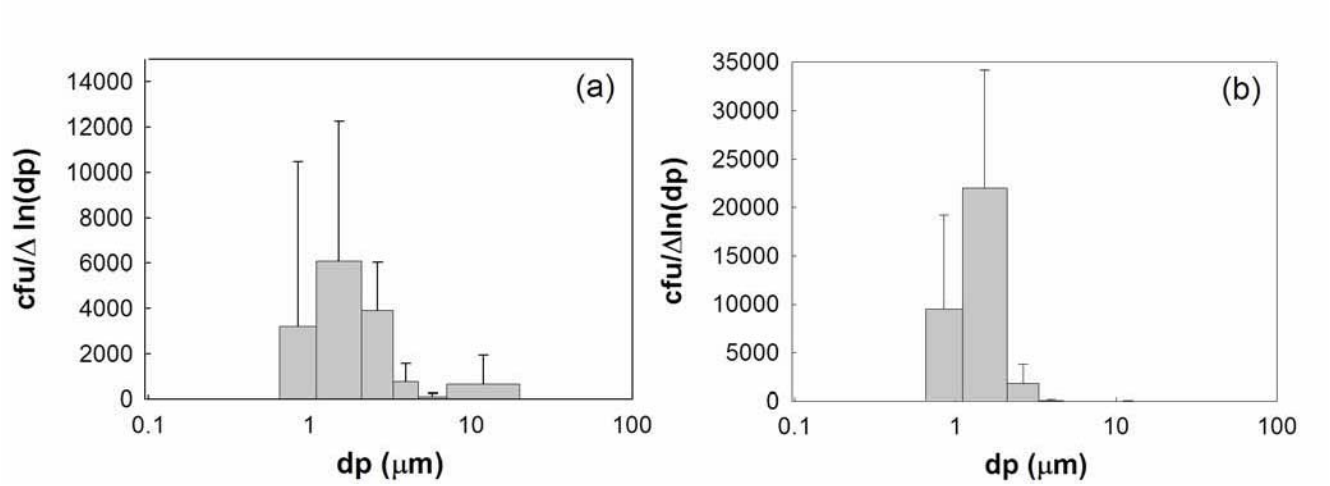

Fig. 5. Size distribution of bioaerosols generated at 15 L/min containing (a) *M. luteus,* and (b) *E. coli.*

PREs greater that 99.8% were observed for the 1.1–2.1 μm particles for all flow rates tested. The result is of similar magnitude to that found in previous studies using N95 filters (Richardson *et al.,* 2006). The efficiency decreased to less than 99% for particles smaller than 0.65 μm and to 96.84% for the iodine-treated filters tested at 15 L/min. Both treated and untreated filters appeared to perform similarly based on the data, which showed no significant difference. The thicker filters (2 mm) appeared to perform better than the regular iodine-treated filters at 15 L/min. This was expected; however, the improvement was relatively slight because the thin filters (1 mm) already demonstrated high capture efficiency.

Pressure drop (Δp) across the filters was recorded. The system was tested with and without the use of the aerosolized particles to determine how particle accumulation on the filter affected Δp. The 1-mm thickness filter had an initial Δp of 0.45 kPa at 15 L/min and 0.57 kPa for 21 L/min. Δp increased as the particles flowed through the testing filters and were subsequently captured.

Pressure drag (S) is a measure of the filter's aerodynamic resistance to air flow. It can be calculated by dividing Δp across a filter by filtration velocity (U) as (Noll, 1999):

$$S = \frac{\Delta p}{U} \tag{2}$$

It is worthwhile noting that the initial pressure drag of the iodinated filters was significantly less than the associated pressure drag of the glass fiber HEPA filters tested, 3.2 kPa·s/m vs. 38 kPa·s/m. Lower filter drag is associated with less-labored respiration, which is beneficial when the mobility of the protected person is critical.

Phase II — Biological disinfection

The size distributions of colony-forming units of the challenged bioaerosols detected at the inlet are shown in Fig. 5. As shown, the majority of the bioaerosol particles generated

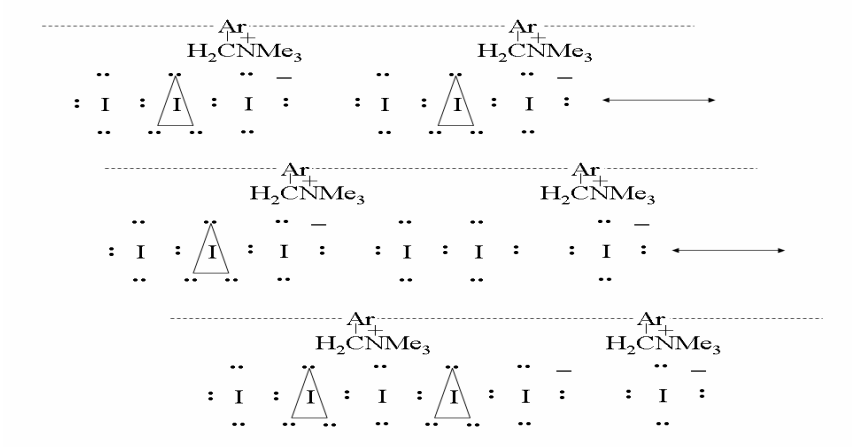

Fig. 6. Canonical limiting structures representing polyiodide complex structure.

were detected in the 1.1–2.1 μm range, which agrees with the nominal size range reported in the literature. The overall vBRE was 99.997 ± 0.004% for *M. luteus* and 99.998 ± 0.005% for *E. coli*. Viable penetration was detected in only two of the 10 experiments. These results indicate that the iodinated resin filters cause close to a 5-log average removal of bioaerosols. The similar vBREs for both species also suggest that the mechanism works for both Gram-positive and Gram-negative species.

The viability of those cells captured on the filter is also of great interest. The vortexing experiments showed no viable cells, further demonstrating the effectiveness of the iodine disinfection mechanism. It should be noted that iodine can be released into solution (0.9 ± 0.03 mg/L in this case) when the iodinated filter is immersed in water. Iodine in water can effectively disinfect those cells as reported in numerous studies (Berg *et al.,* 1964; Black *et al.,* 1968; Marchin *et al.,* 1997). Hence, we can not exclude the possibility that the micro-organisms were deactivated in water rather than on the filter. Nevertheless, both from the low level of penetration and from the intensive contact with iodine at the fiber surface, one can expect the possibility of survival on the filter to be extremely low.

The initial pressure drag of the 1.5-mm thickness filter was less than 10% of that of the glass fiber HEPA filter. Another useful criterion for comparing different types of filters is filter quality, q_F (Hinds, 1999a),

$$q_F = \frac{\ln(1/P)}{\Delta p} \tag{3}$$

where P is the aerosol penetration through the filter. The iodinated medium's filter quality based on the biological removal was 19.9/kPa, which is higher than the glass fiber filter's value, 1.8/kPa. The high efficiency of biological disinfection, zero viable cells on the filter, low pressure drag and high filter quality together demonstrate that the concept of applying a nonspecifically reactive antimicrobial coating to a less-efficient filter offers some significant advantages over conventional HEPA filtration for removing

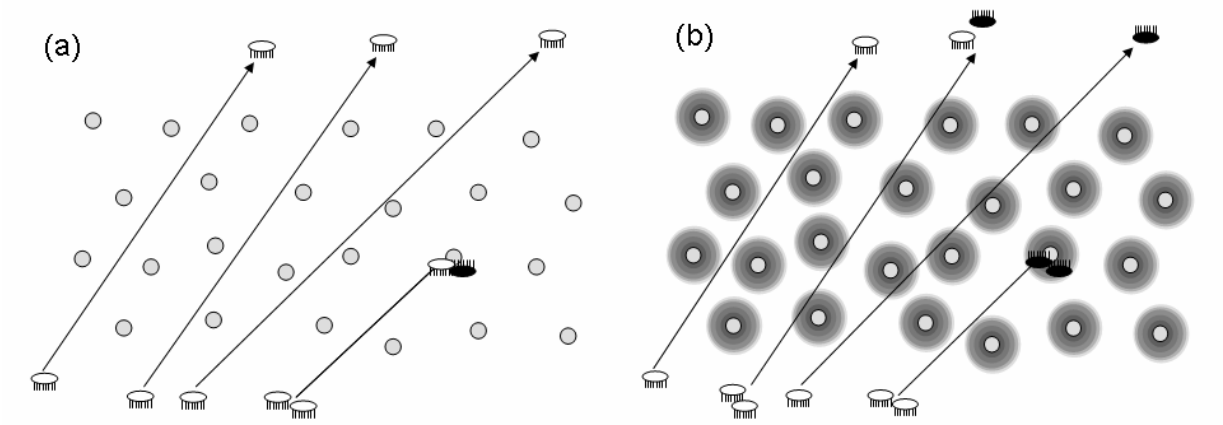

Fig. 7. Proposed mechanism for disinfection: (a) near the untreated, and (b) iodinated polymer, showing notional probability function for capture of I_2 as in Fig. 1 by a microbe passing at minimum distance *x* and comparing outcomes for different minimum distances of approach.

biological agents.

DISCUSSION

The iodine treated filter exhibits a 2-log enhancement of vBRE over PRE, which agrees with previously reported observations of MS2 bioaerosols using similar iodine-treated media (Heimbuch *et al.,* 2004; Heimbuch and Wander, 2006). The enhancement is at least partly due to a demand–release mechanism of the material (Hatch *et al.,* 1980). Hatch *et al.* (1980) proposed three possible mechanisms to explain the phenomenon of demand–release disinfection in water: 1) I_2 release aided by an internal exchange mechanism involving transient formation of higher polyiodide species; 2) hydrolysis of I_2 on the resin to form HOI as the active principle; 3) spontaneous dissociation of I_2 that adheres to the insoluble resin. The scheme in Fig. 6 is drawn by analogy to the reaction of I_3^- with HCN to form ICN and iodide (Edwards *et al.,* 1976), which demonstrates displacement of iodine with concurrent oxidation (demand–release).

The gas–solid system studied here corresponds to the conditions for X-ray crystallography, in which HOI in air has not been reported. So, one may conclude that mechanism 2 is not important for aerosols passing the reactive medium. Mechanism 3 is also suspect because vapor concentrations of I_2 measured downstream of PMT were reported to be < 0.2 mg/m^3 (Di Ionno *et al.,* 2001; Di Ionno and Messier, 2004), and we have measured similar values. In such a short-contact environment, it is difficult to envision a replenishment mechanism fast enough to deliver a lethal dose of I_2 that would not be identical to mechanism 1.

A supportive argument for mechanism 1 also comes from the crystallography cited above and the generalization by Cowie *et al.* (1979) about polyiodide electronic structure and vibrational spectra:

"Molecular I_2 acts as a Lewis acid and coordination to a Lewis base, *e.g.*, I- weakens the I–I bonding. Thus, the I–I distance in I_2 is 2.72 **Å** while in I_3^- it is near 2.92 Å. Molecular orbital calculations on I_3^- also show that the highest occupied molecular orbital has I–I antibonding character."

The simple canonical image (Fig. 6) of PMT that emerges is mobile lines of I_2 molecules and I^- ions (Hatch *et al.,* 1980) in which atoms in the I_2 molecule pass into and out of dsp^3 hybridization as complexes form and dissociate—and from which I_2 molecules can readily be displaced.

Whereas solution disinfection is characterized by long residence times, the aerosol–fiber interaction as a particulate organism traverses the filter matrix is fleetingly transient and the observed efficacy of kill requires that the kinetics of transfer of I_2 be extremely fast—which this visualization allows. Accordingly we propose that near-contact transfer of I_2 occurs from the polyiodide complexes as the bacteria pass near the resin-bound (nominal) I_3^- complex. Fig. 7 displays the concept. A notional probability function for displacement and capture of I_2 —not to be misinterpreted as a concentration gradient of I_2 vapor—from the bound I_3^- complex is illustrated by the graduated intensity of color surrounding the fiber (viewed in cross section). Bacteria are almost universally anionic at their surface. When one passes in proximity to the I_3^- complex on the polymer surface, the distance of closest approach defines the probability that the negative charge on the microbe surface will displace one or more I^- ion(s) and capture an equal number of I_2 molecules. Each captured I_2 molecule then reacts with an iodine-sensitive group on the microbe, and if a critical amount of damage is accumulated the organism ceases to function. Thus, disinfection can occur near but without direct contact with filter surfaces, allowing the carcass to penetrate as an inert particle.

CONCLUSION

In this study, the physical capture and biological disinfection efficiency of a novel biocidal filter medium were evaluated. Significant capture (greater than 97%) by the filters was observed for a wide particle size range. In most cases the efficiency was greater than 99%. There was no discernible difference in the PRE between the iodine-treated and untreated filters, suggesting no mechanical impact of the treatment. The iodinated resin filters were not as efficient at physical removal of aerosols as the glass fiber HEPA filter.

Particles containing two types of microorganisms—*M. luteus* and *E. coli*, which were dominantly in the 1.1–2.1 μm aerodynamic range—were used in the bioaerosol challenge experiments. A simple aqueous dispersant that creates conditions favorable for survival of the organisms in air was employed, rather than the actual or simulated human fluids that one would employ in a study considering factors relating to contagion. vBREs of these two species, representing Gram-positive and Gram-negative bacteria, respectively, were identical, at approximately 99.997%, almost 5-log

attenuation of viable bioaerosols. Indeed, only two of 10 experiments performed showed detectable penetration through the iodine-treated filters. A 2-log enhancement of vBRE over PRE was observed, and we propose a direct mechanism involving displacement and capture of I_2 from the medium. No viable bacterial cells were observed in the vortexing experiments, further supporting the effectiveness of the iodine mechanism to disinfect micro-organisms. The high biological disinfection capacity combined with the low pressure drag and high filter quality demonstrates the novel reactive filter medium to be a viable alternative to conventional filtration for the removal of micrometer bioaerosols. While the filter medium was a disposable unit and was intended for short-term use, information about its effective lifetime is useful and should be investigated in future studies.

ACKNOWLEDGEMENTS

This study was supported by Air Force Research Laboratory under Contract No. F08637-02-C-7030. We would also like to thank the following people for their contributions: Dr. Jean Andino, Arizona State University and the Science Partners for Inquiry Based Learning University of Florida, National Science Foundation for partially providing graduate funding; Dr. George Lukasik, UF Department of Microbiology and Cell Science, University of Florida, for providing cells and protocols; Dr. Ben Koopman, Department of Environmental Engineering Sciences, University of Florida, for providing cells. Finally we are sincerely grateful to the peer reviewer for many constructive suggestions.

REFERNCES

Agranovski, V., Ristovski, Z., Hargreaves, M., Blackall, P.J. and Morawska, L. (2003). Performance Evaluation of the UVAPS: Influence of Physiological Age of Airborne Bacteria and Bacterial Stress. *J. Aerosol Sci.* 34 (12): 1711–1727.

Balazy, A., Toivola, M., Adhikari, A., Sivasubramani, S.K., Reponen, T. and Grinshpun, S.A. (2006). Do N95 Respirators Provide 95% Protection Level Against Airborne Viruses, and How Adequate are Surgical Masks. *Am. J. Infection Ctrl.* 34 (2): 51–57.

Berg, G., Chang, S.L. and Harris, E.K. (1964). Devitalization of Microorganisms by Iodine. *Virology*. 22: 469–481.

Black, A.P., Thomas, W.C., Kinman, R.N., Booner, W.P. and Kein, M.A. (1968). Iodine for the Disinfection of Water. *J. Amer. Water Works Assoc.* 60 (1): 69–83.

Brion, M.G. and Silverstein, J. (1999). Iodine Disinfection of a Model Bacteriophage MS2, Demonstrating Apparent Rebound. *Water Research*. 23: 169–179.

Brosseau, L.M., McCullough, N.V. and Vesley, D. (1997). Mycobacterial Aerosol Collection Efficiency of Respiratory and Surgical Mask Filters Under Varying Conditions of Flow and Humidity. *Appl. Occup. Environ. Hyg*, 12 (6): 435-445.

Carroll, B. (1955). The Relative Germicidal Activities of Triiodide and Diatomic Iodine. *J. Bacteriol.* 69: 413-417.

Chang, S.L. (1958). The Use of Iodine for the Disinfection of Water. *J. Am. Pharm. Assoc.* 48: 417–423.

Cotton, F.A., Wilkinson, G., Murillo, C.A. and Bochmann, M. (1999). *Advanced Inorganic Chemistry*, 6th Ed., John Wiley & Sons, New York, N.Y., pp. 576.

Cowie, M., Gleizes, A., Grynkewich, G.W., Kalina, D.W., McClure, M.S., Scaringe, R.P., Teitelbaum, R.C., Ruby, S.L., Ibers, J.A., Kannewurf, C.R. and Marks, T.J. (1979). Rational Synthesis of Unidimensional Mixed Valence Solids. Structural, Spectral. and Electrical Studies of Charge Distribution and Transport in Partially Oxidized Nickel and Palladium Bisdiphenylglyoximates. *J. Am. Chem. Soc.*, 101 (11): 2921–2936.

Crook, B., Higgins, S. and Lacey, J. (1998). Methods for Sampling Air-Borne Microorganisms at Solid Waste Disposal Sites. *Biodeterioration*. 7: 791–797.

Di Ionno, L. and Messier, P.J. (2004). Iodinated Thermal-Fused Polymer as a Biocidal Additive to Commercial and Chemical-Resistant Coatings. *Surface Coatings International Part B: Coatings Transactions*, 87 (B4): 235–308.

Di Ionno, L., St–Louis, J.P., Bourget, S. and Messier, P.J. An Effective CB Material from Combined Components of Triosyn Resin. *ECBC Scientific Conference on Chemical and Biological Defense Research*, Hunt Valley, Md.

Edwards, J.O., Kaus, M. and Sauer, M.C. (1976). Kinetics of the Reaction of Hydrocyanic Acid with Triiodide Ion. *Inorg. Chem.* 15 (7): 1723–1724.

Fina, L.R., Hassouna, N., Horacek, G.L., Lambert, J.P. and Lambert, J.L. (1982). Viricidal Capability of Resin–Triiodide Demand-Type Disinfectant. *Appl. Environ. Microbiol.* 44 (6): 1370–1373.

Hatch, G.L., Lambert, J.L. and Fina, L.R. (1980). Some Properties of the Quaternary Ammonium Anion-Exchange Resin–Triiodide Disinfectant for Water. *Ind. Eng. Chem. Prod. Res. Dev.* 19: 259–263.

Heimbuch, B., Laventure, G., McDonald, R., Burr, E., Proudfoot, E. and Wander, J. (2004). Antimicrobial Efficiency of Iodinated Individual Protection Filters. *AFRL-ML-TY-TP-2004-4561*, Air Force Research Laboratory, Tyndall AFB, Fla.

Heimbuch, B.K. and Wander, J.D. (2006). Bioaerosol Challenges to Antimicrobrial Surface Treatments: Enhanced Efficacy Against MS2 Coli Phage of Air Filter Media Coated with Polystyrene-4-Methyltrimethylammonium Triiodide. *AFRL-ML-TY-TP-2006-4527*, Air Force Research Laboratory, Tyndall AFB, Fla.

Hinds, W.C. (1999a). *Filtration*. Aerosol Technology: Properties, Behavior, and Measurement of Airborne Particles, John Wiley & Sons, Inc., New York, pp. 183–205.

Hinds, W.C. (1999b). *Production of Test Aerosols.* Aerosol Technology: Properties, Behavior, and Measurement of Airborne

Particles, John Wiley & Sons, Inc., New York, pp. 431.

Jones, G. (1930). On the Existence and Behavior of Complex Polyiodides. *J. Phys. Chem.* 34: 673–691.

Katzin, L.I. and Gerbert, E. (1955). The Iodide-Iodine-Triiodide Equilibrium and Ion Activity Coefficient Ratios. *J. Am. Chem. Soc.* 77: 5814–5819.

Kortepeter, M.G. and Parker, G.W. (1999). Potential Biological Weapons Threats. *Emerging Infectious Diseases*. 5 (4): 523–527.

Lambert, J.L. and Fina, L.R. (1975). *Demand Bactericide for Disinfecting Water and Process of Preparation.* US Patent No. 3923665.

Li, C. and Lin, C.J. (2001). Storage Effects on Bacterial Concentration: Determination of Impinger and Filter Samples. *Sci. Total Environ.* 278: 231–237.

Marchin, G.L., Silverstein, J. and Brion, G.M. (1997). Effect of Microgravity on *Escherichia coli* and MS-2 Bacteriophage Disinfection by Iodinated Resins. *Acta Astronautica*. 40 (1): 65–68.

Maus, R., Goppelsöroder, A., and Umhauer, H. (2000). Survival of Bacterial and Mold Spores in Air and Filter Media. *Atmos. Environ.* 35: 105–113.

May, K.R. (1972). The Collison Nebulizer: Description, Performance and Application. *J. Aerosol Sci.* 4: 235–243.

Messier, P.J. (2000). *Iodine/Resin Disinfection and Procedure for the Preparation Thereof.* US Patent No. 6045820.

Naim, J.O., Lanzafame, R.J., Blackman, J.R. and Hinshaw, J.R. (1986). The in Vitro Quenching Effects of Iron and Iodine on Fluorescein Fluorescence. *J. Surgical Res.* 40: 225–228.

NIOSH. (2005). Determination of Particulate Filter Penetration to Test Against Liquid Particulates for Negative Pressure, Air-Purifying Respirators Standard Testing Procedure (STP). *Procedure No. RCT-APR-STP-0051, 0052, 0053, 0054, 0055, 0056, Revision 1.1*, National Institution for Occupational Safety and Health, National Personal Proctective Technology Laboratory, Pittsburgh, Pa.

Noll, K. (1999). *Fabric Filters.* Fundamentals of Air Quality Systems, American Academy of Environmental Engineers, Annapolis, Md., pp. 173.

Prescott, L., Harley, P.J. and Klein, A.D. (2002). *Microbiology.* McGraw–Hill, New York, N.Y., pp. 147–148, 856, 863.

Qian, Y., Willeke, K., Grinshpun, S.A., Donnelly, J. and Coffey, C.C. (1998). Performance of N95 Respirators: Filtration Efficiency for Airborne Microbial and Inert Particles. *AIHA J.* 59: 128–132.

Rengasamy, S., Verbofsky, R., King, W.P. and Shaffer, R.E. (2007). Nanoparticle Penetration through NIOSH-approved N95 Filtering-facepiece Respirators. *J. Int. Soc. Resp. Protec.* 24: 49–59.

Richardson, A.W., Eshbaugh, J.P., Hofacre, K.C. and Gardner, P.D. (2006). *Respirator Filter Efficiency against Particulate and Biological Aerosols under Moderate to High Flow Rates. ECBC-CR-085*, U.S.

Army Edgewood Chemical Biological Center.

Ruff, I., Friedrich, J. and Csillag, K. (1972). Transfer Diffusion. III. Kinetics and Mechanism of the Triiodide–Iodide Exchange Reaction. *J. Phys. Chem.* 76 (2): 162–165.

Saenger, W. (1984). The Structure of the Blue Starch--Iodine Complex. *Naturwiss.* 71 (1): 31–36.

Swenson, P.H. and Kloo, L. (2002). Synthesis, Structure and Bonding in Polyiodide and Metal Iodide–Iodine Systems. *Chem. Rev.* 103 (5): 1649–1684.

Taylor, S.L., Fina, L.R. and Lambert, J.L. (1970). New Water Disinfectant: an Insoluable Quaternary Ammonium Resin–Triiodide Combination that Releases Bactericide on Demand. *Appl. Microbiol.* 20 (5): 720–722.

Teitelbaum, R.C., Ruby, S.L. and Marks, T.J. (1980). A Resonance Raman/Iodine Mössbauer Investigation of the Starch-Iodine Structure. Aqueous Solution and Iodine Vapor Preparations. *J. Am. Chem. Soc.* 102 (10): 3322–3328.

Vanderpool, R.W., Lundgren, D.A., Marple, V.A. and Rubow, K.L. (1987). Cocalibration of Four Large-Particle Impactors. *Aerosol Sci. Technol.* 7 (2): 177–185.

Vining, G.G. (1998). *Statistical Methods for Engineers, Duxbury Press, Pacific Grove, Calif.*, pp. 309–310.

Wake, D., Bowry, C., Crook, B. and Brown, C. (1997). Performance of Respirator Filters and Surgical Masks Against Bacterial Aerosols. *J. Aerosol Sci.* 28: 1311–1329.

Yu, X., Houtman, C. and Atalla, R.H. (1996). The Complex of Amylose and Iodine. *Carbohydrate Res.* 292: 129–141.

Received for review, August 3, 2007
Accepted, September 24, 2007